Structural Engineering and Mechanics, Vol. 19, No. 2 (2005) 199-215
DOI: http://dx.doi.org/10.12989/sem.2005.19.2.199

An assumed-stress finite element for static and free vibration analysis of Reissner-Mindlin plates

Kutlu Darılmaz†

Department of Civil Engineering, Istanbul Technical University, 34469 Maslak, Istanbul, Turkey

(Received June 7, 2004, Accepted September 16, 2004)

Abstract. An assumed stress quadrilateral thin/moderately thick plate element HQP4 based on the Mindlin/Reissner plate theory is proposed. The formulation is based on Hellinger-Reissner variational principle. Static and free vibration analyses of plates are carried out. Numerical examples are presented to show that the validity and efficiency of the present element for static and free vibration analysis of plates. Satisfactory accuracy for thin and moderately thick plates is obtained and it is free from shear locking for thin plate analysis.

Key words: Reissner-Mindlin plate; hybrid finite element; static analysis; free vibration.

1. Introduction

The early approach to the finite element analysis of plates relied mostly on the Kirchoff thin plate theory, in which transverse shear deformation is neglected. The plate finite element based on this theory requires that the displacement and its derivatives should be continous across element boundaries. This requirement limited the number of possible choices for constructing the interpolation of this kind. Therefore, many works have turned towards the Reissner-Mindlin plate theory (Reissner 1945, Mindlin 1951) as a starting point of the finite element discretization in order to reduce the continuity requirements on the displacement interpolation.

For the Mindlin plates, only C^0 continuity is required, and therefore the difficulties of C^1 continuity requirement for thin plate element are solved easily. Moreover, both thin and thick plate analyses can be integrated into one element model.

All existing Reissner-Mindlin plate elements can be generally classified into two groups. One is displacement-based element method, while the other is the mixed/hybrid element method. In order to avoid the shear locking phenomenon in the displacement-based models, the method of reduced, Zienkiewicz *et al.* (1971), and selective integration, Hughes *et al.* (1978), is an efficient approach to prevent the appearance of the shear locking phenomenon. A number of successful displacement based Reissner-Mindlin plate elements have been developed in recent years, Choi and Park (1999), Wanji and Cheung (2000), Sydenstricker and Landau (2000), Brezzi and Marini (2003), Zengjie and Wanji (2003).

As an alternative to the displacement models, mixed-hybrid models with multiple independent

† Research Assistant (Ph.D), E-mail: kdarilmaz@ins.itu.edu.tr

variables appears to be more attractive in developing thin and thick plate elements. A number of effective elements which are free from shear locking have been developed by authors such as Lee and Pian (1978), Cheung and Wanji (1989), Dong *et al.* (1993), Ayad *et al.* (2001), Ayad and Rigolot (2002) and Eratlı and Akoz (2002). The mixed/hybrid method appears to be an easier technique to satisfy the constraint of the shear strain.

In this paper, an assumed stress hybrid quadrilateral plate element is derived. Reissner-Mindlin theory that incorporates transverse shear deformation is assumed in the plate formulation.

2. Element stiffness formulation

The assumed-stress hybrid method is based on the independent prescriptions of stresses within the element and displacements on the element boundary. The element stiffness matrix is obtained using Hellinger-Reissner variational principle. The Hellinger-Reissner functional of linear elasticity allows displacements and stresses to be varied separately. This establishes the master fields. Two slave strain fields appear, one coming from displacements and one from stresses.

The Hellinger-Reissner functional can be written as

$$\Pi_{RH} = \int_V \{\sigma\}^T[D]\{u\}dV - \frac{1}{2}\int_V \{\sigma\}^T[S]\{\sigma\}dV \tag{1}$$

where $\{\sigma\}$ is the stress vector, $[S]$ is the compliance matrix relating strains, $\{\varepsilon\}$, to stress ($\{\varepsilon\}=[S]\{\sigma\}$), $[D]$ is the differential operator matrix corresponding to the linear strain-displacement relations ($\{\varepsilon\}=[D]\{u\}$) and V is the volume of structure.

$$[S] = \begin{bmatrix} \frac{12}{Eh^3} & -\frac{12\nu}{Eh^3} & 0 & 0 & 0 \\ -\frac{12\nu}{Eh^3} & \frac{12}{Eh^3} & 0 & 0 & 0 \\ 0 & 0 & \frac{24(1+\nu)}{Eh^3} & 0 & 0 \\ 0 & 0 & 0 & \frac{12(1+\nu)}{5Eh} & 0 \\ 0 & 0 & 0 & 0 & \frac{12(1+\nu)}{5Eh} \end{bmatrix} \tag{2}$$

$$[D] = \begin{bmatrix} 0 & \partial/\partial x & 0 \\ 0 & 0 & -\partial/\partial y \\ 0 & \partial/\partial y & -\partial/\partial x \\ \partial/\partial x & 1 & 0 \\ \partial/\partial y & 0 & -1 \end{bmatrix} \tag{3}$$

The approximation for stress and displacements can now be incorporated in the functional. The stress field is described in the interior of the element as

$$\{\sigma\} = [P]\{\beta\} \tag{4}$$

and a compatible displacement field is described by

$$\{u\}=[N]\{q\} \tag{5}$$

where $[P]$ and $[N]$ are matrices of stress and displacement interpolation functions, respectively, and $\{\beta\}$ and $\{q\}$ are the unknown stress and nodal displacement parameters, respectively. Intra-element equilibrating stresses and compatible displacements are independently interpolated. Since stresses are independent from element to element, the stress parameters are eliminated at the element level and a conventional stiffness matrix results. This leaves only the nodal displacement parameters to be assembled into the global system of equations.

Substituting the stress and displacement approximations Eq. (4), Eq. (5) in the functional Eq. (1)

$$\Pi_{RH} = [\beta]^T[G][q] - \frac{1}{2}[\beta]^T[H][\beta] \tag{6}$$

where

$$[H] = \int_V [P]^T[S][P]dV \tag{7}$$

$$[G] = \int [P]^T([D][N])dV \tag{8}$$

Now imposing stationary conditions on the functional with respect to the stress parameters $\{\beta\}$ gives

$$[\beta] = [H]^{-1}[G][q] \tag{9}$$

Substitution of $\{\beta\}$ in Eq. (6), the functional reduces to

$$\Pi_{RH} = \frac{1}{2}[q]^T[G]^T[H]^{-1}[G][q] = \frac{1}{2}[q]^T[K][q] \tag{10}$$

where

$$[K] = [G]^T[H]^{-1}[G] \tag{11}$$

is recognized as a stiffness matrix.

The solution of the system yields the unknown nodal displacements $\{q\}$. After $\{q\}$ is determined, element stresses or internal forces can be recovered by use of Eq. (9) and Eq. (4). Thus

$$\{\sigma\} = [P][H]^{-1}[G]\{q\} \tag{12}$$

Nodal d.o.f. consist of lateral deflections w_i and rotations θ_{xi} and θ_{yi} of midsurface normals so the 4-node HQP4 element (Fig. 1) has 12 d.o.f.s. The corresponding deflections and rotations within an element are obtained by independent shape functions.

The displacement and rotations are expressed in terms of their nodal values and shape functions which are as follows

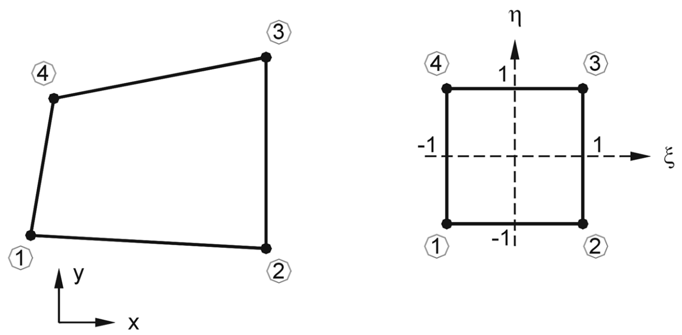

Fig. 1 HQP4 element

$$\{u\} = [N]\{q\} \qquad \{u\}^T = \{w \;\; \theta_x \;\; \theta_y\} \tag{13}$$

$$[N] = \begin{bmatrix} N_1 & 0 & 0 & N_2 & 0 & 0 & N_3 & 0 & 0 & N_4 & 0 & 0 \\ 0 & N_1 & 0 & 0 & N_2 & 0 & 0 & N_3 & 0 & 0 & N_4 & 0 \\ 0 & 0 & N_1 & 0 & 0 & N_2 & 0 & 0 & N_3 & 0 & 0 & N_4 \end{bmatrix} \tag{14}$$

$$N_i = \frac{1}{4}(1 + \xi\xi_i)(1 + \eta\eta_i) \quad \text{for} \quad i = 1, 2, 3, 4 \tag{15}$$

where i denotes the node number.

Coordinates x and y within the element are defined by

$$x = \sum N_i x_i \quad \text{and} \quad y = \sum N_i y_i \tag{16a}$$

By the relations between the global Cartesian coordinate system (x, y) and the normalized nodal coordinate system (ξ, η), matrix J is defined as

$$[J] = \begin{bmatrix} \partial x/\partial\xi & \partial y/\partial\xi \\ \partial x/\partial\eta & \partial y/\partial\eta \end{bmatrix} = \begin{bmatrix} \sum N_{i,\xi}\, x_i & \sum N_{i,\xi}\, y_i \\ \sum N_{i,\eta}\, x_i & \sum N_{i,\eta}\, x_i \end{bmatrix} \tag{16b}$$

Initial polynomials are usually assumed for the stresses after which the equilibrium equations are applied to these polynomials yielding relations between the β's and ultimately the final form of [P]. The equilibrium equations which are applied to stress field polynomials yielding relations between the β's are given in Eq. (17).

$$\begin{aligned} \frac{\partial M_x}{\partial x} + \frac{\partial M_{xy}}{\partial y} - Q_x &= 0 \\ \frac{\partial M_y}{\partial y} + \frac{\partial M_{xy}}{\partial x} - Q_y &= 0 \\ \frac{\partial Q_x}{\partial x} + \frac{\partial Q_y}{\partial y} &= 0 \end{aligned} \tag{17}$$

The biggest difficulty in deriving hybrid finite elements seems to be the lack of a rational methodology for deriving stress terms, Feng *et al.* (1997). It is recognized that the number of stress modes m in the assumed stress field should satisfy

$$m \geq n - r \tag{18}$$

with n the total number of nodal displacements, and r the number of rigid body modes in an element. If Eq. (18) is not satisfied, use of too few coefficients in $\{\beta\}$, the rank of the element stiffness matrix will be less than the total degrees of deformation freedom and the numerical solution of the finite element model will not be stable and produces on element with one or more mechanism.

Increasing the number of β's by adding stress modes of higher-order term, each extra term will add more stiffness and stiffen the element, Pian and Chen (1983), Punch and Atluri (1984).

The element has 12 d.o.f, three of which are associated with the out of plane rigid body motions. Therefore, a stress field with a minimum of 9 independent parameters is needed to describe the stress field.

The assumed stress field for the plate element which satisfies the equilibrium conditions (Eq. 17) for zero body forces and avoids rank deficiency is given as

$$\begin{aligned} M_x &= \beta_1 + \beta_4 y + \beta_6 x + \beta_8 xy \\ M_y &= \beta_2 + \beta_5 x + \beta_7 y + \beta_9 xy \\ M_{xy} &= \beta_3 + \beta_{10} x + \beta_{11} y + \beta_{12} x^2/2 + \beta_{13} y^2/2 \\ Q_x &= \beta_6 + \beta_{11} + \beta_8 y + \beta_{13} y \\ Q_y &= \beta_7 + \beta_{10} + \beta_9 x + \beta_{12} x \end{aligned} \tag{19}$$

Numerical experimentations indicate that these 13 parameter selections of stress field are somewhat more accurate and less sensitive to geometric distortion than fewer parameter selections. This selection of stresses produces no spurious zero energy modes. It is observed stress field remains invariant upon node numbering.

3. Element mass matrix

The problem of determination of the natural frequencies of vibration of a plate reduces to the solution of the standard eigenvalue problem $[K] - \omega^2[M] = 0$, where ω is the natural angular frequency of the system. Making use of the conventional assemblage technique of the finite element method with the necessary boundary conditions, the system matrix $[K]$ and the mass matrix $[M]$ for the entire structure can be obtained.

Element mass matrix is derived from the kinetic energy expression

$$E_k = \frac{1}{2}\int_A \{\dot{q}\}^T [R] \{\dot{q}\} dA \tag{20}$$

where $\{\dot{q}\}$ denotes the velocity components and $[R]$ is the inertia matrix.

$$[R] = \begin{bmatrix} \rho h & 0 & 0 \\ 0 & \rho\frac{h^3}{12} & 0 \\ 0 & 0 & \rho\frac{h^3}{12} \end{bmatrix} \tag{21}$$

The nodal and generalized velocity vectors are related with the help of shape functions

$$\{\dot{q}\} = \sum_{i=1}^{4}[N]\{\dot{q}_i\} \tag{22}$$

Substituting the velocity vectors in the kinetic energy, Eq. (20) yields the mass matrix of an element.

$$E_k = \frac{1}{2}\int_A \{\dot{q}_i\}^T[N]^T[R][N]\{\dot{q}_i\}dA \tag{23}$$

$$E_k = \frac{1}{2}\int_A \{\dot{q}_i\}^T[m]\{\dot{q}_i\}dA \tag{24}$$

where $[m]$ is the element consistent mass matrix and is given by

$$[m] = \int_A [N]^T[R][N]dA \tag{25}$$

4. Numerical examples

Some standard numerical examples have been used for assessing the accuracy of the HQP4 element. The results obtained are compared with analytic and some other element solutions that are available in open literature.

Example 1: Absence of spurious modes: examination of the stiffness matrix rank

The eigenvalues of the stiffness matrix $[K]$ for one element are computed for different values of the thickness and for various shapes of the element. Three zero eigenvalues corresponding to the three rigid body motions of a plate are always obtained, showing thus a proper rank for the matrix $[K]$ and the absence of spurious modes in consequence. Three sample elements are depicted in Fig. 2.

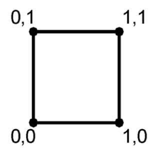

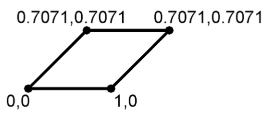

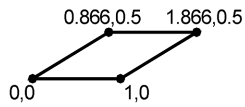

Thickness	1	0.1	0.01	1	0.1	0.01	1	0.1	0.01
# zero eigenvalues of [K]	3	3	3	3	3	3	3	3	3
Rank[G]	9	9	9	9	9	9	9	9	9

Fig. 2 Number of zero eigenvalues

Example 2: Simply supported square plate

The classical test problem of a simply supported square plate under uniform loading is considered. The plate is made of linear elastic isotropic material with Elasticity modulus E = 10.92 kN/m^2 and Poissons's ratio ν = 0.3. The side length a = 10 m and different h/a values are selected. The numerical results are obtained by modeling one quadrant using uniform finite element meshes given in Fig. 3.

The results obtained for h/a = 0.001 (thin) to h/a = 0.2 (moderately thick) values are presented in Table 1 and results showed that the behaviour of the HQP4 element is satisfactory, converges to the analytical value. The analytical solution is extracted from Timoshenko and Woinowsky-Krieger (1959).

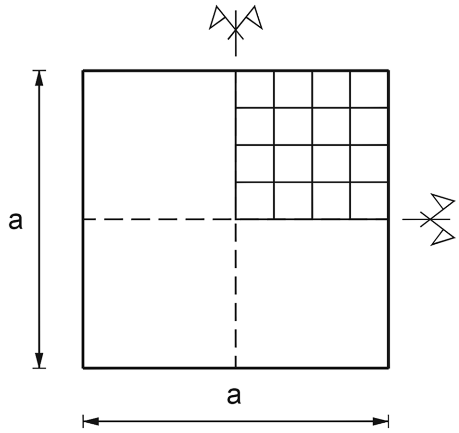

Fig. 3 Uniform loading on a simply supported square plate

Table 1 Displacement parameter ($w_{max}Eh^3/pa^4$) at the centre of uniformly loaded simply supported square plate

	h/a			
	0.001	0.05	0.1	0.2
HQP4 (This study)	0.04445	0.04504	0.04678	0.05376
Pryor *et al.* (1970)	---	0.04469	0.04612	0.05186
Rao *et al.* (1974)	---	0.04483	0.04627	0.05201
Bhashyam, Gallagher (1983)	---	0.04510	0.04760	0.05690
Bergan, Wang (1984)	---	-	0.04663	0.05296
MITC4 Bathe, Dvorkin (1985)	---	---	---	0.05344
Yuan, Miller (1989)	0.04396	0.04636	0.05015	0.06045
MITC9 (Bathe *et al.* 1989)	0.04436	---	---	---
Akoz, Uzcan (1992)	---	0.0450	-	0.0520
Q4Bla (Xu *et al.* 1994)	---	---	0.04728	---
Wanji, Cheung (2000)	---	0.04485	---	0.05338
Analytical	0.04436	0.04486	0.04632	0.05360

Example 3: Uniform loading on a rhombic plate

The rhombic plate model selected in this example given in Fig. 4 is made of linear elastic material with Elasticity modulus $E = 10 \times 10^6$ kN/m^2, Poisson's ratio ν = 0.3, plate side a = 100 m and plate thickness h = 1 m. The solution for the center displacement under unit uniform load q = 1 kN/m^2, analytical solution obtained by Morley (1963), is used for comparison with numerical results.

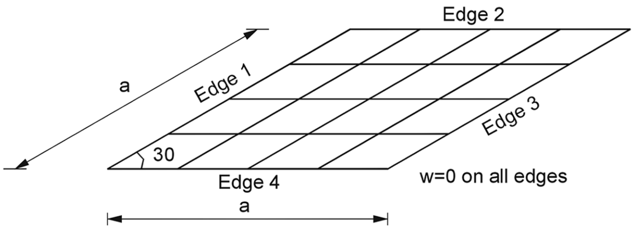

Fig. 4 Uniform loading on a simply supported rhombic plate

Table 2 Displacements at the centre of uniformly loaded simply supported rhombic plate

	Mesh			
	2 × 2	4 × 4	8 × 8	16 × 16
HQP4 (This study)	0.03984	0.04160	0.04137	0.04361
Q4-R (Malkus and Hughes 1978)	---	0.04509	0.04433	0.04477
DKQ (Batoz, Tahar 1982)	0.20804	0.08303	0.05533	0.04835
T1 (Hughes, Tezduyar 1989)	0.02780	0.03918	0.03899	0.04187
Ibrahimbegovic (1993)	0.04627	0.04271	0.03971	0.04206
Q4BL (Zienkiewicz *et al*. 1993)	---	0.05606	0.04807	
RDKQM (Wanji, Cheung 2000)	---	0.08266	0.05503	0.04816
RDKTM* (Wanji, Cheung 2001)	---	0.04958	0.04641	0.04597
ANSYS	0.07601	0.05082	0.04669	0.04528
Analytical (Morley 1963)	0.04455	0.04455	0.04455	0.04455

*Triangular element

Results showed that the behaviour of the HQP4 element is satisfactory, converges to the analytical value.

Example 4: Uniform loading on a circular plate

The Fig. 5 shows the geometry and finite element mesh used for the analysis of an isotropic moderately thick ($R/h = 5$) and thin ($R/h = 50$) circular plate subjected to a $q = 1$ kN/m^2 uniform loading. The radius is chosen as R = 5 m and the material properties are Elasticity modulus $E = 10 \times 10^6$ kN/m^2, Poisson's ratio $\nu = 0.3$. This problem is interesting owing to the arbitrarily distorted mesh.

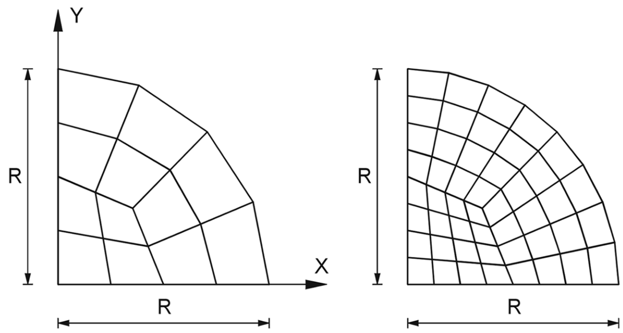

Fig. 5 Uniform loading on a simply supported and clamped circular plate

A quarter of a plate with symmetry conditions on x and y axes is discretized using 12 and 48 elements. Two types of boundary conditions are considered:

SS: Simply supported plate with $w = 0$ on the boundary

CL: Clamped plate with $w = \theta_x = \theta_y = 0$ on the boundary

The analytical solutions for displacement w and moment M at the centre including transversal shear effects are obtained for axisymmetric plates as follows, Ayad and Rigolot (2002).

Simply supported plate $\quad w_{ref} = \dfrac{qR^4}{64D}\left(\dfrac{\nu+5}{\nu+1}+\phi\right) \qquad M_{ref} = \dfrac{qR^2}{16}(\nu+3)$

Clamped plate $\quad w_{ref} = \dfrac{qR^3}{64D}(1+\phi) \qquad M_{ref} = \dfrac{qR^2}{16}(\nu+1)$

Where

$$\phi = \frac{8}{3k(1-\nu)}\left(\frac{h}{R}\right)^2 \qquad D = \frac{Eh^3}{12(1-\nu^2)} \qquad k = \frac{5}{6}$$

The results are presented in Table 3 with the results obtained by other researchers and analytical solution.

Table 3 Central deflection of clamped circular plate (uniform load)

	R/h = 5		*R/h* = 50	
	12	48	12	48
HQP4 (This study)	11.076	11.432	9296	9612
Q4-R (Malkus and Hughes 1978)	11.125	11.405	9392	9641
MITC4 (Bathe, Dvorkin 1985)	11.421	11.529	9693	9769
Ibrahimbegovic (1993)	11.367	11.505	---	---
Q4BL (Zienkiewicz *et al.* 1993)	10.760	---	9003	---
Q4Bla (Xu *et al.* 1994)	10.927	11.399	9115	9628
RDKQM (Wanji, Cheung 2000)	11.748	11.604	10079	9870
Akoz, Eratlı (2000)	11.561*	11.549**	9792*	9781**
Analytical	11.551	11.551	9784	9784

*15 sectorial elements, **54 sectorial elements

Table 4 Bending moment M_x at the center of clamped circular plate

	R/h = 5		*R/h* = 50	
	12	48	12	48
HQP4 (This study)	2.060	2.029	2.061	2.029
Q4-R (Malkus and Hughes 1978)	1.967	2.015	2.010	2.035
MITC4 (Bathe, Dvorkin 1985)	2.046	2.033	2.075	2.031
Q4BL (Zienkiewicz *et al.* 1993)	1.910	---	1.910	---
Q4Bla (Xu *et al.* 1994)	1.965	2.017	1.692	2.009
RDKQM (Wanji, Cheung 2000)	2.178	2.070	2.149	2.064
Akoz, Eratlı (2000)	2.277*	2.047**	2.595*	1.960**
Analytical	2.031	2.031	2.031	2.031

*15 sectorial elements, **54 sectorial elements

Table 5 Central deflection of simply supported circular plate (uniform load)

	R/h = 5		R/h = 50	
	12	48	12	48
HQP4 (This study)	40.039	40.997	37915	39236
Q4-R (Malkus and Hughes 1978)	38.787	40.912	37052	39148
MITC4 (Bathe, Dvorkin 1985)	40.766	41.395	39037	39634
Ibrahimbegovic (1993)	42.201	41.750	---	---
Q4BL (Zienkiewicz *et al.* 1993)	41.744	---	40007	---
Q4Bla (Xu *et al.* 1994)	41.722	41.644	39899	39871
RDKQM (Wanji, Cheung 2000)	41.093	41.470	39423	39735
Akoz, Eratlı (2000)	41.220*	41.192**	39858*	39840**
Analytical	41.599	41.599	39831	39831

*15 sectorial elements, **43 sectorial elements

Table 6 Bending moment M_x at the center of simply supported circular plate

	R/h = 5		R/h = 50	
	12	48	12	48
HQP4 (This study)	5.128	5.136	5.186	5.158
Q4-R (Malkus and Hughes 1978)	4.935	5.095	5.004	5.151
MITC4 (Bathe, Dvorkin 1985)	5.098	5.139	5.124	5.137
Q4BL (Zienkiewicz *et al.* 1993)	5.121	---	5.121	---
Q4Bla (Xu *et al.* 1994)	5.169	5.164	5.101	5.152
RDKQM (Wanji, Cheung 2000)	5.229	5.176	5.201	5.170
Akoz, Eratli (2000)	5.192*	5.163**	5.205*	5.163**
Analytical	5.156	5.156	5.156	5.156

*15 sectorial elements, **43 sectorial elements

Results showed that the behaviour of the HQP4 element is satisfactory, converges to the reference value.

Example 5: Natural frequencies of a square plate

The natural frequencies of a square plate with three different support conditions are determined. Dimensions and material properties of the plate are taken for each case as h = 0.15 m, E = 25000 Mpa, ν = 0.15, a = 10 m, ρ = 24 kN/m^3. In Table 7, Table 8 and Table 9 the values of the non-dimensional

Table 7 Non-dimensional frequency ϖ_{mn} for a square plate simply supported on four edges

Frequency Parameters	Leissa (1973)	Omurtag *et al.* (1997)	Eratlı, Akoz (2002)	Wang *et al.* (2004)	ANSYS (Shell63)	HQP4 (This study)
ϖ_{11}	19.739	19.911	19.703	19.739	19.653	19.812
ϖ_{12}	49.348	50.112	49.069	49.348	48.993	48.337
ϖ_{21}	49.348	50.112	49.069	49.348	48.993	48.337
ϖ_{22}	78.957	80.090	78.354	78.957	77.750	81.764
ϖ_{31}	98.696	---	---	98.694	97.870	98.382
ϖ_{32}	98.696	---	---	98.694	97.870	98.382

Table 8 Non-dimensional frequency ϖ_{mn} for a square plate clamped on four edges

Frequency Parameters	Leissa (1973)	Omurtag *et al.* (1997)	Eratlı, Akoz (2002)	Wang *et al.* (2004)	ANSYS	HQP4 (This study)
ϖ_{11}	35.999	36.018	35.931	35.985	35.623	35.696
ϖ_{12}	73.405	74.497	73.823	73.393	72.372	72.683
ϖ_{21}	73.405	74.497	73.823	73.393	72.372	72.683
ϖ_{22}	108.237	108.949	110.14	108.22	105.388	106.361
ϖ_{31}	131.64	---	---	131.57	129.528	130.268
ϖ_{32}	132.24	---	---	132.19	130.364	130.842

Table 9 Non-dimensional frequency ϖ_{mn} for a square cantilever plate

Frequency Parameters	Zienkiewicz (1971)	ANSYS	HQP4 (This study)
ϖ_{11}	3.469	3.472	3.463
ϖ_{12}	8.535	8.544	8.517
ϖ_{21}	21.450	21.357	21.309
ϖ_{22}	27.059	27.226	27.114
ϖ_{31}	---	31.156	30.195
ϖ_{32}	---	54.550	52.917

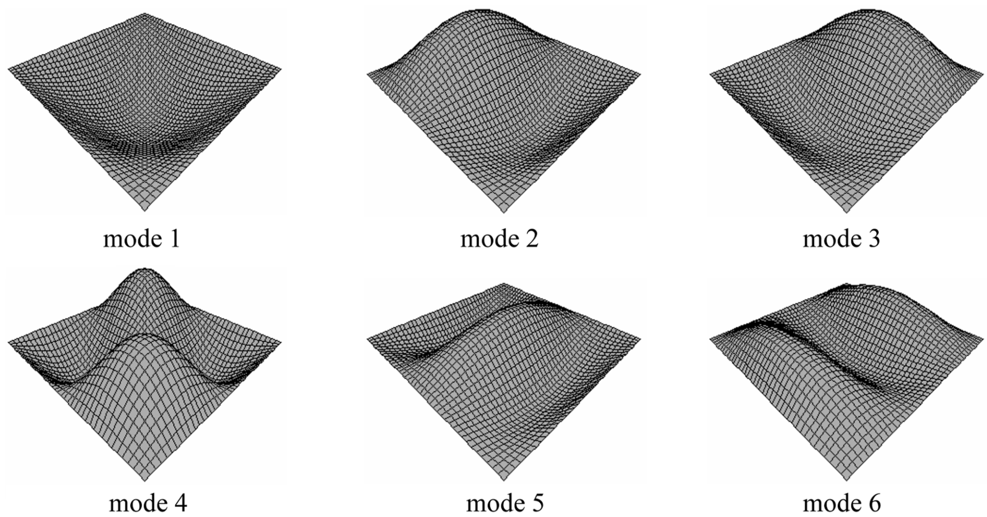

Fig. 6 First six modes of the square plate simply supported on four edges

frequencies ϖ_{mn} ($\varpi_{mn} = \omega_{mn} a^2 \sqrt{\rho h / D}$) obtained by some other researchers are given together with the HQP4 results for comparison.

The first six mode shapes of the simply supported, clamped and cantilever plate are depicted in Fig. 6, Fig. 7 and Fig. 8, respectively.

Results showed that the behaviour of the HQP4 element is satisfactory and results are in a good agreement with other solutions.

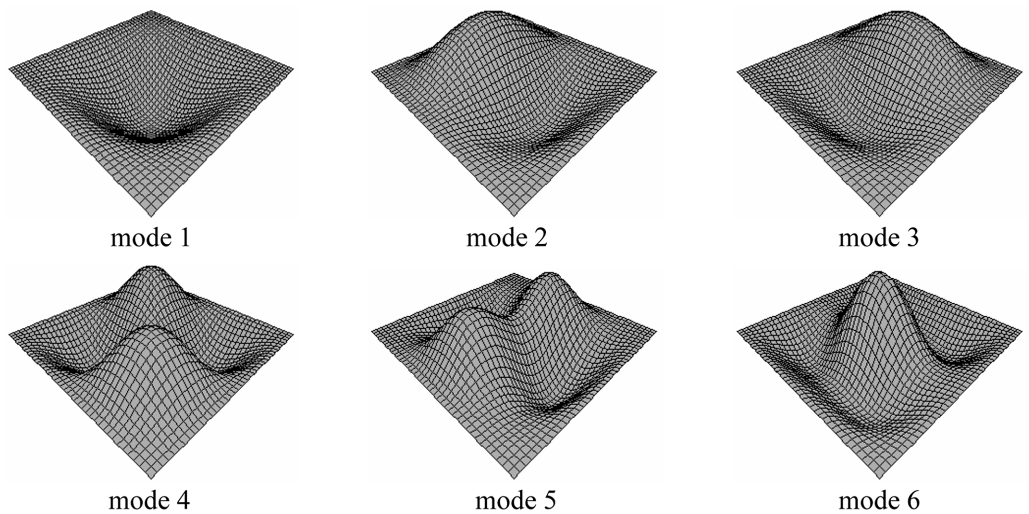

Fig. 7 First six modes of the square plate clamped on four edges

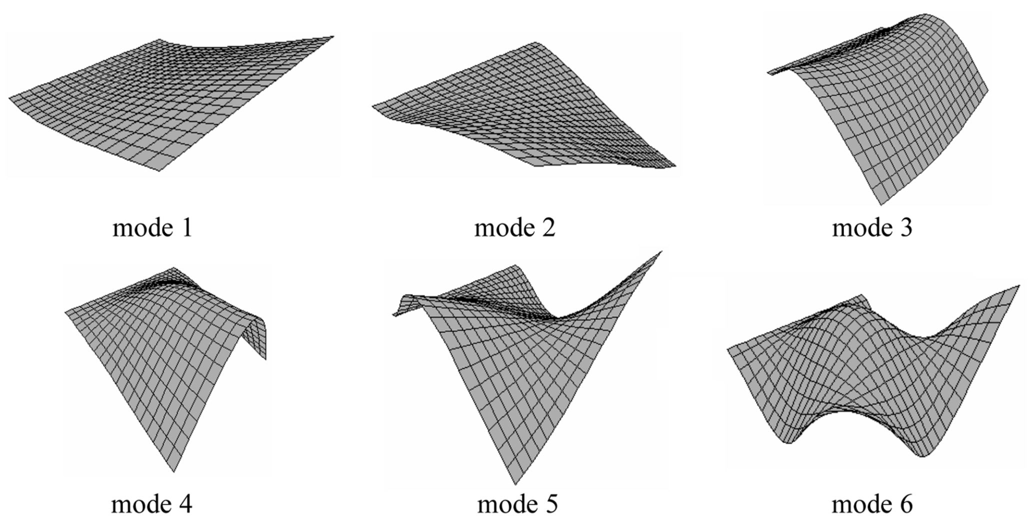

Fig. 8 First six modes of the square cantilever plate

Example 6: Natural frequencies of a rhombic plate

To validate the accuracy of presented finite element model, the frequency parameter $\lambda = (\omega_{mn}a^2/\pi^2)\sqrt{\rho h/D}$ of a rhombic plate with different support conditions has been determined. The dimensions and material properties are the same with the plate given in Example 3, except the thickness of plate. h = 20 (h/a = 0.2) is used for this example.

In Table 10 the values of the non-dimensional frequencies obtained by Woo *et al.* and ANSYS solutions are given together with the HQP4 results for comparison.

Results obtained are in a good agreement with the ANSYS and element solutions presented in Woo *et al.* (2003).

Table 10 Frequency parameter $\lambda = (\omega_{mn} a^2/\pi^2)\sqrt{\rho h/D}$ for the rhombic plate with various edge conditions

Edge condition	Mode number	HQP4 (This study)	Woo *et al.* (2003)	ANSYS
CCCC	1	6.423	6.238	5.932
	2	8.331	8.070	8.681
	3	9.914	9.643	11.395
	4	12.011	11.376	13.885
	5	12.193	11.543	14.303
	6	14.971	---	17.295
CSCS	1	5.603	5.506	5.689
	2	7.597	7.429	7.717
	3	9.328	9.103	9.617
	4	11.201	10.875	11.481
	5	11.605	11.344	11.859
	6	12.973	---	13.374
FCFC	1	3.647	3.560	3.761
	2	3.692	3.635	3.789
	3	5.616	5.501	5.836
	4	6.704	6.456	6.907
	5	8.012	7.740	8.449
	6	9.082	---	9.320
FFFC	1	0.483	0.479	0.489
	2	1.351	1.342	1.419
	3	2.265	2.243	2.464
	4	2.969	2.941	3.142
	5	4.187	4.142	4.436
	6	5.371	---	5.693

Example 7: Natural frequencies of a circular plate

A circular plate with a simply supported (w = 0 at edges) boundary condition is considered. The dimensions and material properties are the same with the plate given in Example 4. Nondimensionalized frequencies, $\omega r^2\sqrt{\rho h/D}$, where r is the radius, are computed for such a circular plate with different thickness/diameter ratios. In Table 11, the first six nondimensionalized frequencies are shown and compared with other solutions. Obviously, a good agreement has been obtained for the thin cases.

The first six mode shapes of the circular plate are depicted in Fig. 9.

Table 11 Nondimensionalized frequencies $\omega r^2\sqrt{\rho h/D}$ for a simply supported circular plate

$h/2r$	Mode number	HQP4 (This study)	Wiberg *et al.* (1994)	ANSYS	Thin plate solution Leissa and Narita (1980)
0.2	1	4.497	4.405	4.508	4.9352
	2	10.91	10.49	10.85	13.8982
	3	10.91	10.49	10.85	13.8982
	4	17.22	16.62	17.07	25.6133
	5	17.25	16.63	17.10	25.6133
	6	19.33	19.01	19.47	29.72

Table 11 Continued

$h/2r$	Mode number	HQP4 (This study)	Wiberg *et al.* (1994)	ANSYS	Thin plate solution Leissa and Narita (1980)
0.1	1	4.799	4.779	4.809	4.9352
	2	12.898	12.66	12.895	13.8982
	3	12.898	10.67	12.895	13.8982
	4	22.304	21.81	22.269	25.6133
	5	22.352	21.82	22.288	25.6133
	6	25.664	25.35	25.989	29.72
0.01	1	4.915	4.932	4.921	4.9352
	2	13.84	13.88	13.84	13.8982
	3	13.84	13.89	13.84	13.8982
	4	25.37	25.53	25.37	25.6133
	5	25.39	25.55	25.42	25.6133
	6	29.70	29.96	29.64	29.72

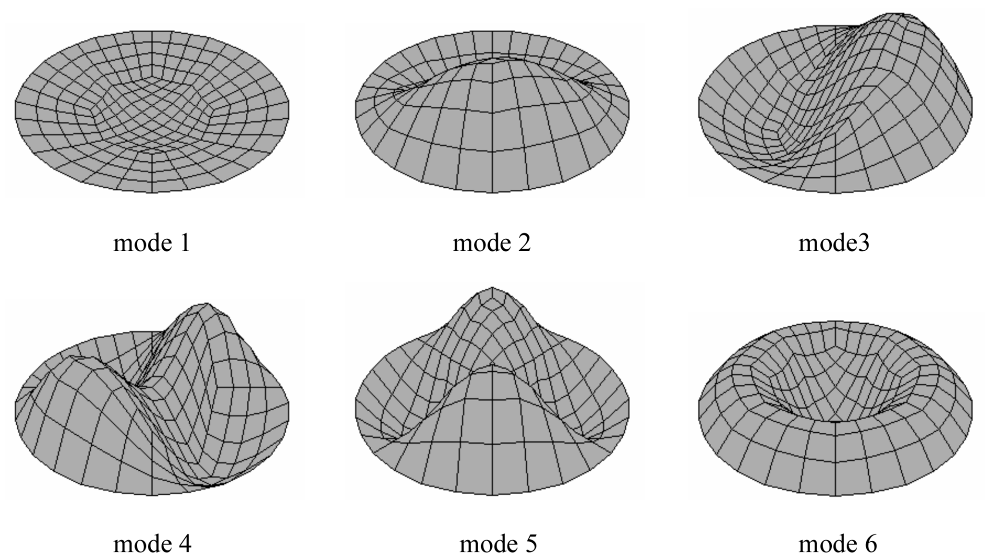

Fig. 9 First six modes of the circular plate

6. Conclusions

The main goal of this study is to investigate the performance of the HQP4 element in static and free vibration analysis of thin to moderately thick plates. A number of numerical problems are utilized to assess the performance of the present element. Numerical comparisons show that the present element yields comparatively satisfactory results and does not exhibit shear locking. The behaviour in case of element distortion deviates but is still in general qualitatively comparable.

Acknowledgements

The author gratefully acknowledge the excellent support and encouragement provided by Professor Dr. Nahit Kumbasar.

References

Akoz, A.Y. and Uzcan, N. (1992), “The new functional for Reissner plates and its application”, *Comput. Struct.*, **44**(5), 1139-1144.

Akoz, A.Y. and Eratlı, N. (2000), “A sectorial element based on Reissner plate theory”, *Struct. Eng. Mech.*, **9**(6), 519-540.

ANSYS (1997), Swanson Analysis Systems, Swanson J. ANSYS 5.4. USA.

Ayad, R., Rigolot, A. and Talbi, N. (2001), “An improved three-node hybrid-mixed element for Mindlin/Reissner plates”, *Int. J. Num. Meth. Eng.*, **51**(8), 919-942.

Ayad, R. and Rigolot, A. (2002), “An improved four-node hybrid-mixed element based upon Mindlin’s plate theory”, *Int. J. Num. Meth. Eng.*, **55**, 705-731.

Bathe, K.J. and Dvorkin, E.H. (1985), “A four-node plate bending element based on Mindlin/Reissner plate theory and mixed interpolation”, *Int. J. Num. Meth. Eng.*, **21**, 367-383.

Bathe, K.J., Brezzi, F. and Cho, S.W. (1989), “The MITC7 and MITC9 plate bending elements”, *Comput. Struct.*, **32**(3-4), 797-814.

Batoz, J.L. and Tahar, M.B. (1982), “Evaluation of a new quadrilateral thin plate bending element”, *Int. J. Num. Meth. Eng.*, **18**, 1655-1677.

Bergan, P.G. and Wang, X. (1984), “Quadrilateral plate bending elements with shear deformations”, *Comput. Struct.*, **19**(1-2), 25-34.

Bhashyam, G.R. and Gallagher, R.H. (1983), “A triangular shear flexible finite element for moderately thick laminated composite plates”, *Comp. Methods Appl. Mech. Eng.*, **40**, 309-326.

Brezzi, F. and Marini, L.D. (2003), “A nonconforming element for the Reissner-Mindlin plate”, *Comput. Struct.*, **81**(8-11), 515-522.

Choi, C.K. and Park, Y.M. (1999), “Quadratic NMS Mindlin-Plate-Bending Element”, *Int. J. Num. Meth. Eng.*, **46**, 1273-1289.

Cheung, Y.K. and Wanji, C. (1989), “Hybrid quadrilateral element based on Mindlin-Reissner plate theory”, *Comput. Struct.*, **32**(2), 327-339.

Dong, Y.F., Wu, C.C. and Defreitas, J.A.T. (1993), “The hybrid stress model for Mindlin-Reissner plates based on a stress optimization condition”, *Comput. Struct.*, **46**(5), 877-897.

Eratlı, N. and Akoz, A.Y. (2002), “Free vibration analysis of Reissner plates by mixed finite element”, *Struct. Eng. Mech.*, **13**(3), 277-298.

Feng, W., Hoa, S.V. and Huang, Q. (1997), “Classification of stress modes in assumed stress elds of hybrid finite elements”, *Int. J. Num. Meth. Eng.*, **40**, 4313-4339.

Hughes, T.J.R., Cohen, M. and Haroun, M. (1978), “Reduced and selective integration techniques in finite element analysis of plates”, *Nuc. Eng. Des.*, **46**, 203-222.

Hughes, T.J.R. and Tezduyar, T.E. (1981), “Finite elements based upon Mindlin plate theory with particular reference to the four-node bilinear isoparametric element”, *J. Appl. Mech.*, **46**, 587-596.

Ibrahimbegovic, A. (1993), “Quadrilateral finite elements for analysis of thick and thin plates”, *Comput. Meth. Appl. Mech. Eng.*, **110**, 195-209.

Lee, S.W. and Pian, T.H.H. (1978), “Improvement of plate and shell finite-elements by mixed formulations”, *AIAA J.*, **16**(1), 29-34.

Leissa, A.W. (1973), “The free vibration of rectangular plates”, *J. Sound Vib.*, **31**, 257-293.

Malkus, D.S. and Hughes, T.J.R. (1978), “Mixed finite element methods-reduced and selective integration techniques: a unification of concepts”, *Comput. Meth. Appl. Mech. Eng.*, **15**, 63-81.

Mindlin, R.D. (1951), “Influence of rotatory inertia and shear on flexural motion of isotropic, elastic plates”, *J.*

Appl. Mech., ASME, **18**, 31-38.
Morley, L.S.D. (1963), *Skew Plates and Structures, Series of Monographs in Aeronautics and Astronautics*, MacMillan, New York.
Omurtag, M.H., Ozutok, A. and Akoz, A.Y. (1997), "Free vibration analysis of Kirchhoff plates resting on elastic foundation by mixed finite element formulation based on Gateaux differential", *Int. J. Num. Meth. Eng.*, **40**(2), 295-317.
Pian, T.H.H. and Chen, D.P. (1983), "On the suppression of zero energy deformation modes". *Int. J. Num. Meth. Eng.*, **19**, 1741-1752.
Pryor, C.W., Jr., Barker, R.M. and Frederick, D. (1970), "Finite element bending analysis of Reissner plate", *J. Eng. Mech. Div.* ASCE, **96**, 967-983.
Punch, E.F. and Atluri, S.N. (1984), "Development and testing of stable, isoparametric curvilinear 2 and 3-D hybrid stress elements", *Comput. Meth. Appl. Mech. Eng.*, **47**, 331-356.
Rao, G.V., Venkataramana, J. and Raju, I.S. (1974), "A high precision triangular plate bending element for the analysis of thick plates", *Nuc. Eng. Des.*, **30**, 408-412.
Reissner, E. (1945), "The effect of transverse shear deformation on the bending of plates", *J. Appl. Mech.*, ASME, **12**, A69-A77.
Sydenstricker, R.M. and Landau, L. (2000), "A study of some triangular discrete Reissner-Mindlin plate and shell elements", *Comput. Struct.*, **78**(1-3), 21-33.
Timoshenko, S.P. and Woinowsky-Krieger, S. (1959), *Theory of Plates and Shells* (2nd edn). McGraw-Hill: New York.
Wang, Y.L., Wang, X.W. and Zhou, Y. (2004), "Static and free vibration analyses of rectangular plates by the new version of the differential quadrature element method", *Int. J. Num. Meth. Eng.*, **59**(9), 1207-1226.
Wanji, C. and Cheung, Y.K. (2000), "Refined quadrilateral element based on Mindlin/Reissner plate theory", *Int. J. Num. Meth. Eng.*, **47**(1-3), 605-627.
Wanji, C. and Cheung, Y.K. (2001), "Refined 9-dof triangular Mindlin plate elements", *Int. J. Num. Meth. Eng.*, **51**, 1259-1281.
Woo, K.S., Hong, C.H., Basu, P.K. and Seo, C.G. (2003), "Free vibration of skew Mindlin plates by *p*-version of F.E.M.", *J. Sound Vib.*, **268**, 637-656.
Xu, Z., Zienkiewicz, O.C. and Zeng, L.F. (1994), "Linked interpolation for Reissner-Mindlin plate elements: Part III- An alternative quadrilateral", *Int. J. Num. Meth. Eng.*, **37**, 1437-1443.
Yuan, F. and R. Miller E. (1989), "A cubic triangular finite element for flat plates with shear", *Int. J. Num. Meth. Eng.*, **28**, 109-126.
Zengjie, G. and Wanji, C. (2003), "Refined triangular discrete Mindlin flat shell elements", *Comput. Mech.*, **33**(1), 52-60.
Zienkiewicz, O.C. (1971), *The Finite Element Method in Engineering Science*, McGraw-Hill.
Zienkiewicz, O.C., Taylor, R.L. and Too, J.M. (1971), "Reduced integration technique in geneal analysis of plates and shells", *Int. J. Num. Meth. Eng.*, **3**, 275-290.
Zienkiewicz, O.C., Xu, Z., Zeng, L.F., Samuelsson, A. and Wiberg, N.E. (1993), "Linked interpolation for Reissner-Mindlin plate elements: Part I- A simple Quadrilateral", *Int. J. Num. Meth. Eng.*, **36**, 3043-3056.

Notations

a	: length of the plate edge
h	: thickness of plate
E	: modulus of elasticity
G	: shear modulus of elasticity
D	: flexural rigidity of the plate
M_x, M_y, M_{xy}	: internal moment components
Q_x, Q_y	: internal shear force components
q	: distributed load
R	: radius

λ	: frequency parameter
ν	: Poisson ratio
ρ	: mass per unit volume
ω	: natural angular frequency
ϖ	: non-dimensional frequency
$[D]$	: differential operator matrix
$[G]$	: nodal forces corresponding to assumed stress field
$[N]$	: shape functions
$[R]$	: inertia matrix
$[P]$	: interpolation matrix for stress
$\{q\}$, $\{\dot{q}\}$	: displacement and velocity components
$\{u\}$	: displacements
$\{\beta\}$	: stress parameters
$\{\sigma\}$	: internal forces